
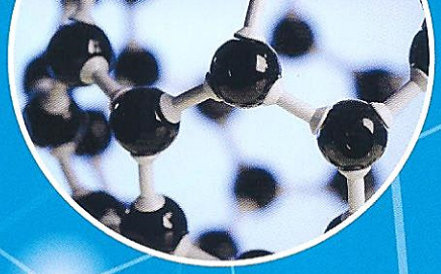


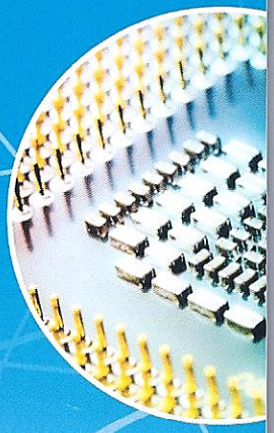

June 14-17, 2015
Washington, DC
Gaylord National Hotel
& Convention Center

TechConnect World Innovation Conference & Expo

NANOTECH
CONFERENCE & EXPO

NATIONAL INNOVATION
SUMMIT & SHOWCASE

NATIONAL SBIR/STTR
CONFERENCE

Business Program - pg. 26
Full Conference Program - pg. 48

TechConnect Platinum Sponsors

AUTODESK.

BASF
We create chemistry

nationalgrid

NSTXL
NATIONAL SECURITY TECHNOLOGY ACCELERATOR

In Partnership with

NSTI
Nano Science and Technology Institute

Produced by

TechConnect
#TCInnovation

Raman Spectroscopic Characterization of Carbon Nanotubes & Tungsten Oxide of Relevance to Energy Storage and Gas Sensing Applications

P. Misra[*], D. Casimir[*], R. Garcia-Sanchez[*] and S. Baliga[**]

[*]Howard University, Department of Physics & Astronomy, Washington, DC, USA pmisra@howard.edu
[**]General Monitors, An MSA Company, Lake Forest, CA, USA, ShankarB@Generalmonitors.com

ABSTRACT

The characterization of graphitic and metal oxide nanomaterials through the use of Resonant Raman Spectroscopy at multiple laser excitations is the primary aim of this research. Raman spectroscopic techniques can help characterize the vibrational phonon modes of nano-materials with little in the way of sample preparation, making it an ideal tool for device characterization. The Stokes Raman spectra of carbon nanotubes and tungsten oxide were recorded with a DXR Smart Raman spectrometer over a temperature range of 27-200 degrees Celsius. The Raman spectra of SWCNTs were used to demonstrate the bond softening and resultant red-shifting of the various Raman peaks of SWCNTs. The thermal changes in the spectra were used to characterize the nanomaterial samples with an eye to future applications for energy storage (using carbon nanotubes) and for toxic gas sensing (using tungsten oxide). The observed and modeled red-shifting of the Raman frequencies and broadening of the peak widths are being used to better understand the thermo-mechanical response of the nanomaterials for potential device applications at elevated temperatures.

Keywords: Raman spectroscopy, Tungsten Oxide, Carbon Nanotube, Chirality, Radial Breathing Mode

1 INTRODUCTION

Resonance Raman spectroscopy has become one of the most common techniques in the characterization of single walled carbon nanotubes (SWCNT) and other nanomaterials. It is possible to obtain rich, detailed Raman spectra from samples with little to no work in the way of sample preparation, in contrast to more expensive scanning probe methods, e.g. AFM & TEM. Understanding of the thermal expansion properties of carbon nanotubes provides potential insight into the process of storing thermal energy in these materials. Meanwhile, metal oxide gas sensors work by bringing about a change in conductivity in the sensor due to gas exposure caused by the chemisorption of oxygen. We have investigated these processes in which molecules are adsorbed into the metal oxide lattice structure with the goal of understanding how the Raman spectral features change as a result of varying conditions, especially temperature effects. The Raman spectroscopy data were recorded using a ThermoFisher DXR (532 nm and 780 nm) Smart Raman spectrometer and a Renishaw inVia Raman Microscope (514 nm).

2 RAMAN SPECTROSCOPY OF CARBON NANOTUBES

In this section, the unique Raman signatures and electronic structure of SWCNTs will be described. A discussion on the use of these features – besides the exploitation of the similarities in the Raman spectra of SWCNT and other graphitic materials - in the identification of and characterization of these nanomaterials follows.

2.1 Carbon Nanotube Raman Spectral Features

The unique electronic density of states of single-walled carbon nanotubes (SWCNTs) is responsible for a many-fold increase in Raman intensities, which are usually weak in other nanomaterial samples. The diameter-dependence of the optical transition levels responsible for the resonant enhancement of SWCNT Raman intensities may also be used in the determination of the chiralities present in one's sample. First, however, we describe the various Raman bands present in SWCNT and other carbon allotropes. The first order feature at approximately 1580 cm^{-1} (denoted as the G-band) represents the E_{2g} Raman active mode, which is the vibrational motion of the C-atoms in the hexagonal graphitic unit cell that is restricted to the plane of the graphene sheet [1]. Besides the doublet nature in SWCNT, this Raman peak is common to all sp^2 hybridized graphitic materials, hence its designation as the G, or "Graphite" first order band. The two components of the doublet nature of the G-band in SWCNT are caused by the strain associated with the rolling up of the conceptual parent material, the graphene sheets, in the formation of nanotubes. The lower portion designated by ω_G^- at ~1560cm^{-1} may be used to determine whether or not the resonant nanotube is of metallic or semiconducting character. In the case of semiconducting SWCNT, this lower part of the doublet, which is associated with vibrational motion in the circumferential direction of the nanotube, has a Lorentzian line-shape that is equal in width to its higher frequency counterpart, ω_G^+ [2]. The ω_G^- feature that is associated with metallic SWCNT, however, has a much broader Breit Wigner Fano peak, with a lower center frequency [3]. The current candidate explanation for the

broadening and down-shifting of the ω_G^- band for metallic SWCNT is the interaction between the tangential mode phonons and surface plasmons [4].

Another Raman band that is again common to all sp^2 carbon allotropes is the peak that ranges from ~1250 – 1450 cm^{-1}. This band, known as the "Defect" or D-band, is associated with certain vibrational modes brought about by effects that lower the crystalline symmetry of the respective material, which may include atom vacancies, grain boundaries, finite size effects, and any other defects that diminish the symmetries of quasi-infinite perfect regular lattices. This Raman feature can be used, with caution, in assessing sample quality [5]. Two other features from the Raman spectrum of SWCNT that should be carefully considered when using the D-band for defect characterization are the small line-widths, anywhere from 7-40 cm^{-1}, and the fact that the Raman spectra of bundled SWCNT samples are usually composed of broad peaks that are composed from the superposition of multiple peaks from many single walled nanotubes that are close in diameter [6].

The peak around ~2574 cm^{-1} known as the G' band is also characteristic of sp^2 hybridized carbon allotropes. This feature which ranges from anywhere between 2500-2800 cm^{-1} results from a second order scattering process involving the activation of a Raman active phonon near the K point in graphene's Brillouin zone via a double resonance process [6]. The important differences in this feature applicable for the characterization of graphite and graphene are the peak location and shape. The G' peak for the graphite sample is at a higher frequency of 2725 cm^{-1} as compared to that of the graphene sample at 2685 cm^{-1}. The interaction between graphene layers is responsible for the frequency upshift in the former material [7]. The G' band of the graphene sample is also symmetric, while that of the graphite sample has a noticeable shoulder. As expected, the numerous Lorentzian contributions in the fitting of this peak for graphite are linked to the interaction of the vibrational modes of the several graphene layers.

2.2 Radial Breathing Mode

The Radial Breathing Mode band of single walled carbon nanotubes is a peak which occurs in the low frequency range around ~120-300cm^{-1}. It is unique to carbon nanotubes, and as its name suggests, it refers to the coherent vibration of the carbon nanotube as a whole in the radial direction, as if the tube is breathing [8]. The appearance of this Raman peak, in addition to the previously discussed bands, allows one to conclude that carbon nanotubes are definitely present in one's sample. This Raman mode was also recognized early in carbon nanotube research to be inversely proportional to the SWCNT diameter, with numerous researchers exploiting this relationship in the estimation of tube diameter via Eqn (1).

$$\omega_{RBM} = \frac{A}{d_t} + B \tag{1}$$

Sauvajol, et. al. in reference [9] made a careful study of this relationship in light of the difficulties in obtaining individually separated SWCNTs, and in accounting for the effects of van der Waals interactions in the determination of the parameters A and B in the application of equation 1 to Raman data from bundled SWCNT samples. The values of A and B determined in Sauvajol et al's study were 238.0 cm^{-1} nm and ~ 0 cm^{-1}, respectively. A very useful master curve, relating the RBM frequency and inverse diameter for bundled nanotube samples, was also developed by the authors, as shown in Fig. 10 of reference [9].

2.3 Effect of Temperature on the Raman Spectra of SWCNT

Studies have shown that increased temperature causes a red-shift in the frequency of many of the Raman features of SWCNTs [4]. According to these studies, this frequency shift occurs due to both a thermal effect and a volume effect caused by the thermal expansion of the lattice. Equation 2 summarizes these two effects:

$$\Delta\omega = \left(\frac{\partial\omega}{\partial T}\right)_V \Delta T + \left(\frac{\partial\omega}{\partial V}\right)_T \left(\frac{\partial V}{\partial T}\right)_P \Delta T \tag{2}$$

Based on previous studies, we know that the thermal effect dominates, while the volume effects are negligible. Equation 3 shows the temperature dependence of the frequency of the Raman feature (in the case of Fig. 2, the RBM peak), where ω_0 is the fitted frequency linearly extrapolated to 0K, and a_1 represents the first order temperature coefficient, respectively. Figure 1 is a plot of the radial breathing mode vs. temperature data demonstrating the previously mentioned dominance of the pure temperature effect due to phonon interactions.

$$\omega = \omega_0 - a_1 T \tag{3}$$

Figure 2 shows the temperature variation of the fractional volume change, and Fig. 3 shows the volume coefficient of thermal expansion β of an actual SWCNT sample used in our study, that were obtained using the temperature-induced shift of the radial breathing mode . It can be seen from Fig. 3 that based on the thermally shifted RBM the bundled SWCNT sample's volume CTE decreases from $0.2*10^{-6}$ to $-0.5*10^{-7}K^{-1}$ over the temperature range 300-473K.

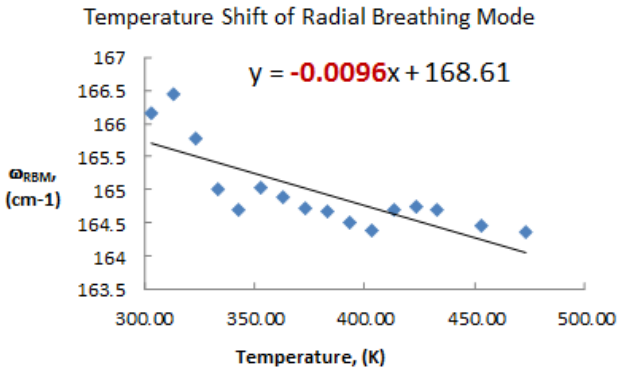

Figure 1. Temperature variation of the Radial Breathing Raman mode of SWCNT sample.

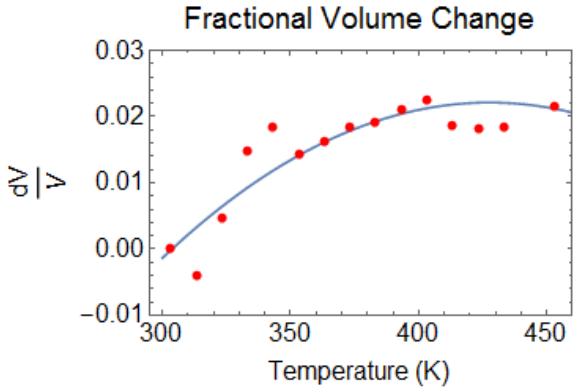

Figure 2. Calculated temperature variation of the fractional volume change of the SWCNT sample using the data from Fig. 1.

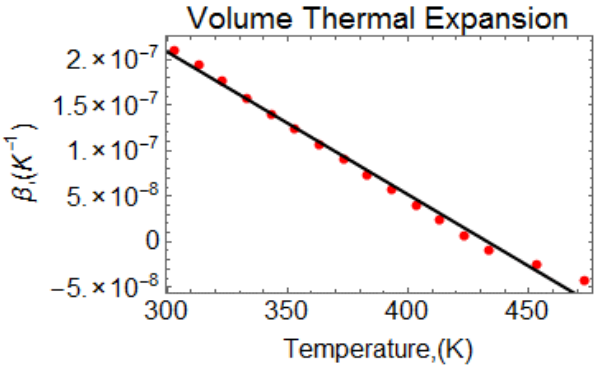

Figure 3. Calculated temperature variation of the volume coefficient of thermal expansion of SWCNT sample.

3 RAMAN SPECTROSCOPY OF METAL OXIDE GAS SENSORS

In this section, we will discuss the Raman spectroscopy research on metal oxide gas sensors, mainly WO_3 variants, and how their Raman spectral features undergo changes based on increasing/decreasing temperatures, primarily focused in the 25°C-200°C temperature range using 780 nm wavelength laser excitation. We have previously studied the behavior of temperature increases in the range 30°C-160°C [11]. In this paper we discuss the effects of lowering the temperature, going from 190°C to 30°C, and the different effects the cycles have on the Raman spectroscopy of tungsten oxide.

4 WO_3 RAMAN SPECTRAL FEATURES

We have focused our investigations strictly on the monoclinic form of WO_3 on a silicon substrate. The main features for monoclinic WO_3 are seen around ~807, ~716, and ~271 cm^{-1}, which correspond to the stretching of O-W-O bonds, stretching of W-O and the bending of O-W-O, respectively. Figure 4 illustrates the Raman spectral signature of WO_3 for 532 nm (top) and 780 nm (bottom) excitation wavelengths, respectively. Several other Raman peaks can be seen corresponding to other vibrations of W-O and O-W-O bonds. The peak around ~1550 cm^{-1} corresponds to OH-O and W-OH, which is a result of humidity effects on the sample. A complete listing of peak assignments as related to multiple WO_3 features can be found in our previously published study [11].

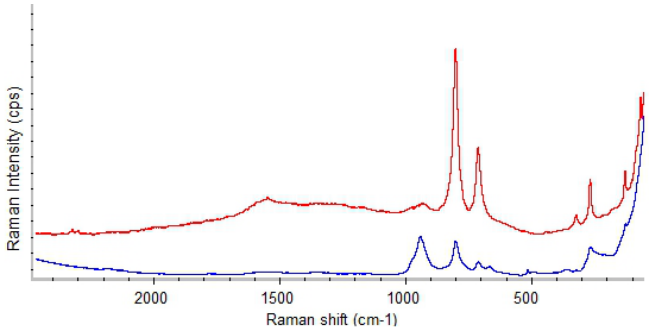

Figure 4. Raman Spectrum of WO3 at 30°C using 532 nm wavelength (top) and 780 nm (bottom).

5 EFFECT OF TEMPERATURE AND HUMIDITY STUDIES ON THE RAMAN SPECTRA OF WO_3

During our studies relating to increasing temperature [11], we found that the Raman spectra of a variety of nanomaterial samples, namely WO_3 on silicon, WO_3 nanopowder and WO_3 nanowires, exhibited changes as the temperature increased. We noted that certain features disappeared as temperature increased, potentially related to oscillations of the O-H feature around ~1550 cm^{-1}, an effect caused by humidity. In addition, shifts occurred in the wavenumbers of these features and are illustrated in Fig. 5. Figure 5 shows the case of lowering temperature (190°C to 30°C), and we find that just as the O-H vibrations become more pronounced with increasing temperature, reducing temperature decreases these O-H vibrations too.

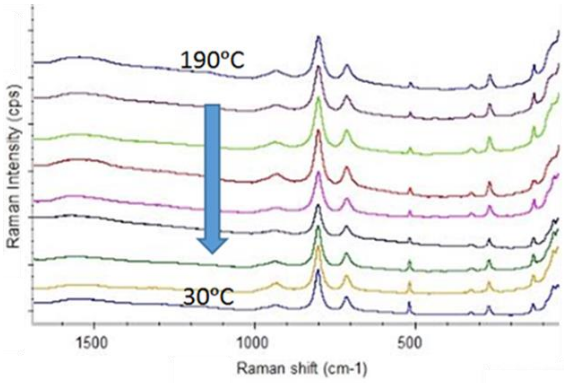

Figure 5. The Raman spectra of WO3 on Si with decreasing temperature from 190°C (top spectrum) to 30°C (bottom spectrum) at intervals of 20°C.

6 CONCLUSIONS

The present proceedings paper discusses how Raman spectroscopy, a powerful minimally invasive optical technique, has been proven to be an effective characterization technique for studying nanomaterials. Specifically, we have been able to determine quantitatively the temperature shifts in the frequencies of the Raman spectral features that are associated with carbon nanotubes (CNTs) and tungsten oxide (WO_3). Concurrently, classical Molecular Dynamics simulation was used in the structural characterization of these nanomaterials. Indeed, the resulting redshift in the Raman features of SWCNTs is a direct consequence of this thermal effect. Thermal expansion, in turn, is related to concepts of thermal energy storage and further work in this regard is in progress. The need to create a feasible method of assessing the thermo-mechanical response and ensuing strain in carbon nanotubes will be a critical operational parameter in future applications of these materials. In addition to these thermal effects related to SWCNTs, we have also observed a measurable shift in the frequencies of the WO_3 Raman peaks with increasing and decreasing temperatures. We are currently studying the correlation between the thermal effects in SWCNTs and WO_3.

REFERENCES

1. F. Tuinstra and J.L. Koenig, Journ. Chem. Phys. **53**, 1126 (1970), doi: 10.1063/1.1674108.
2. M.S. Dresselhauss, G. Dresselhauss, A. Jorio, A.G. Souza Filho, R. Saito, Carbon **40**, 2043-2061 (2001).
3. A. Jorio, R. Saito, G. Dresselhauss, M.S. Dresselhauss, *Raman Spectroscopy in Graphene Related Systems* (Wiley-VCH Verlag GmbH & Co. KGaA, Weinheim, Germany, 2011).
4. M.S. Dresselhauss and P.C. Eklund, Advances in Physics **49**, 705-814 (2000).
5. R. Saito et al., Advances in Physics **60**, no. 3, 413-550 (2011).
6. P. Misra, D. Casimir, and R. Garcia-Sanchez, "Thermal Expansion Properties of Single-Walled Carbon Nanotubes by Raman Spectroscopy at 780 nm wavelength," Annual International Conference on Optoelectronics, Photonics & Applied Physics (OPAP) 2013 Proceedings.
7. Joe Hodkiewicz, Thermo Fisher Scientific Application Note: 51901, Thermo Fisher Scientific, Madision, WI, USA.
8. A. Jorio et al., New Journal of Physics **5**, 139.1-139.17 (2002).
9. J-L. Sauvajol, E. Anglaret, S. Rols, and L. Alvarez, Carbon **40**, 1697-1714 (2002).
10. S.J. Stuart, A.B. Tutein, J.A. Harrison, J. Chem. Phys. **112**, 6472-6486 (2000).
11. R. Garcia-Sanchez, T. Ahmido, D. Casimir, S. Baliga, P. Misra, J. Phys. Chem. A **117**, 13825-13831 (2013), Special Issue: Terry A. Miller Festschrift, doi: 10.1021/jp408303p.